文章编号:1004-7220(2011)02-0181-08

Reevaluation on the mechanical properties of dentine microstructure

LUO Xiao-song[1], ZHANG Yi-xia[2], CUI Yu-hong[1], PAN Jun[3] (1. *Department of Mechanics, Tianjin University, Tianjin* 300072, *China*; 2. *School of Engineering and Information Technology, University of New South Wales, Australian Defence Force Academy, Canberra, ACT* 2600, *Australia*; 3. *College of Bioenginerring, Chongqing University, Chongqing* 400044, *China*)

Abstract: Objective It is demostrated that the porous protein-mineral mechanics model could provide more accurate prediction for biomaterial properties of dentine compared with the other established models. This paper would use the model to re-evaluate the mechanical properties and its interacting mechanism of human dentine. **Method** By using a porous protein-mineral mechanics model, the effect from the interactions between tubules, peritubular and intertubular matrix on dentine microstructure was discussed. **Results** The dentinal micromechanical properties were dependent on the tubular direction, and the absolute values of the stresses derived from the hydraulic and gas tubular pressures increased parabolically with the increasing diameter of the tubules. It was also found that the effective elastic constants of the dentine microstructure would vary with the aging and the distribution of mineral and collagen within peritubular and intertubular matrix of detine. **Conclusions** The theoretical analyses provided in this paper demonstrated that the microstructural characteristics of tubules, peritubular and intertubular dentinal matrix could have different influences on the micromechanical properties of human dentine, which showed the validity of porous protein-mineral mechanics model, and the limitation of some models that neglected the interacting mechanism.

Key words: Mechanical properties; Dental materials; Microstructure; Reevaluation

牙本质微结构性质的重新评价

罗晓松[1], 张义霞[2], 崔玉红[1], 潘 君[3]
(1. 天津大学 力学系, 天津 300072; 2. 澳大利亚新南威尔士大学国防分校 工程与信息技术学院, 堪培拉 ACT2600;
3. 重庆大学 生物工程学院 重庆 48044)

摘要: 目的 相比以前一些模型,蛋白质-矿物质多孔力学模型被验证可以提供更精确的生物材料性质评价。因此,本文对牙本质微结构相互作用对其材料性质的影响进行了重新评价。**方法** 采用蛋白质-矿物质多孔力学模型,讨论了牙小管、管周基质和管间基质相互作用对牙本质微结构性质的影响。**结果** 通过分析发现,牙本质微结构力学性质依赖于牙小管的方向和牙小管中的压力值;同时,牙本质微结构力学性质会随着年龄以及管周基质与管间基质的蛋白质和矿物质分布而改变。**结论** 文章中的理论分析和讨论说明牙小管、管周基质和管间基质相互作用对牙本质微结构性质有一定的影响,说明蛋白质-矿物质多孔力学模型的有效性,以及不考虑相互作用的微结构力学模型具有一定的局限性。

关键词: 力学性质; 牙本质; 微结构; 重新评价
中图分类号: R 3 **文献标志码:** A

Dentine is an important structural component of human teeth. Recent studies on the mechanical properties of dentine from different laboratories are highly inconsistent[1-2]. Some researchers explain that the inconsistency of the me-

收稿日期: 2010-05-14; **修回日期:** 2010-07-09
基金项目: 国家自然科学基金资助项目(308706060)。
通讯作者: 崔玉红, Tel: (022)81774927; E-mail: yhcui@tju.edu.cn。

chanical properties among different lab tests is caused by the microstructure of dentine, a classical anisotropic porous biotissue, which is composed of tubules, intertubular dentine, and peritubular dentine. It has been found that the elastic properties of a dentine microstructure are influenced by many factors such as different wet and dry conditions[1,3-4], the direction of the tubule[1,3,5-7], hydraulic and gas pressures in tubular dentine[8], the aging of dentine[7,9-11], and the distributions of mineral and collagen[11-12].

Although some laboratory works have been carried out recently, there are few studies on the analytical or numerical analysis on the micromechanics of the dentine. The mechanics models developed in most of the previous studies on the dentinal microstructural properties are based on imperforate fiber composite and isotropic homogenized assumption by Christensen, Voigt and Reuss, Huo and Zheng[1-2,5-6,8,13-17]. However, the porosity of dentinal materials has not been taken into account completely in those models, such as the model developed by Kinney *et al.*[5]; the model proposed by Qin *et al.*[8], which is originated from the self-consistent method[13]; the work of Huo *et al.*[6,16], which was based on effective self-consistent method; and the hexagonal-array model based on strain energy approach[17].

The objective of this study is to use a new micromechanics model developed by the authors to evaluate the mechanical properties and interacting mechanism of the dentine microstructure[18-19]. In this model, the anisotropic constitutive relations and the interactions among tubules, intertubular dentine, and peritubular dentine are considered. By using the new model, the interacting mechanism of mechanical properties of the dentine microstructure including factors such as angular dependence, different wet and dry conditions, aging, mineral and collagen distributions of human dentine, and hydraulic and gas tubular pressure, have been studied. The theory and model developed in this study have been finally validated by numerical examples.

1 Materials and Methods

1.1 The porous protein-mineral micromechanics model

The microstructure of normal human dentin is usually composed of three parts: a tubule with gas or liquid in the middle of the microstructure; a peritubular cuff reinforcing phase of carbonated apatite; and an intertubular cuff mostly consisting of type I collagen (Fig. 1)[1-2]. In normal dentine, the tubules are lined with a highly mineralized peritubular cuff, and the collagen fibrils formed intertubular dentin matrix is arranged in a felt-like structure and oriented perpendicular to the tubules[4,9]. In light of a classic dentine microstructure, the authors have proposed a porous protein-mineral mechanics model as shown in Fig. 1(a) and 1(b)[6,18], in which the tubule represents the porosity; the intertubular dentine cuff represents the protein section; and the mineralized cuff of the peritubular dentine represents the mineral section. Fig. 1(b) shows a unit cell of microsrtucture dentin with an AFM (atomic force microscope) image of full dentine specimens shown on the left and the mechanics model shown on the right[1]. In Fig. 1(b), a is the radius of the microstructural tubule; b is the total radius of the microstructural intertubular and peritubular dentine; and c is the total radius of the whole dentine microstructure. $\alpha = a/b$ represents the ratio of tubule area to the area of the intertubular and peritubular dentine; $\beta = b/c$ represents the ratio of the area of intertubular and peritubular dentine to the gross area.

Most previous models assume isotropic dentine microstructure and sparse distribution of the dental tubules. Measurement of the elastic constants for human dentine by resonant ultrasound spectroscopy demonstrates that the microstructure has a slight hexagonal anisotropy, and a hexagonal symmetry model agrees well with the predicted material properties obtained from the measurement[3,18]. A transverse section of a porous protein-mineral mechanics model with hexagonal shape is shown in Fig. 1(c), and the model under P_0 and P_1 pressures is shown in Fig. 1(d), where P_0 represents the inside stress from gas and liquid pressures, and P_1 represents the outside stress caused by the interactions among the representative volume elements[18]. In the porous protein-mineral model, the interactive effects among different sections of dentine microstructure have been taken into account based on the general self-consistent method[14,18], and this model is employed in this study for investigating the interacting mechanism of mechanical properties of the dentine microstructure.

1.2 Representative volume element and constitutive relationship

A representative volume element should be large enough and contain adequate tubules to represent the trans-

versely isotropic property of dental material. It has been reported that the reasonable microscopic finding for the model could be obtained with seven or more unit cells according to experiment (Fig. 1(c))[3]. The constitutive equation of the representative volume element of hexagonal transversely isotropic symmetry model can be presented as following[19]:

$$\begin{bmatrix}\sigma_{11}\\ \sigma_{22}\\ \sigma_{33}\\ \sigma_{12}\\ \sigma_{23}\\ \sigma_{31}\end{bmatrix}=\begin{bmatrix}C_{11} & C_{12} & C_{12} & 0 & 0 & 0\\ C_{12} & C_{22} & C_{23} & 0 & 0 & 0\\ C_{12} & C_{23} & C_{22} & 0 & 0 & 0\\ 0 & 0 & 0 & 2C_{44} & 0 & 0\\ 0 & 0 & 0 & 0 & C_{22}-C_{23} & 0\\ 0 & 0 & 0 & 0 & 0 & 2C_{44}\end{bmatrix}\begin{bmatrix}\varepsilon_{11}\\ \varepsilon_{22}\\ \varepsilon_{33}\\ \varepsilon_{12}\\ \varepsilon_{23}\\ \varepsilon_{31}\end{bmatrix} \quad (1)$$

Where $\sigma_{ij}, \varepsilon_{ij}$ ($i,j=1,2,3$) are the components of stress and strain; C_{ij} are the elastic constants for the model, i.e.:

$$E_{11}=C_{11}-\frac{2C_{12}}{C_{22}+C_{23}}$$

$$G_{12}=G_{13}=G_1=C_{44}$$

$$G_{23}=\frac{1}{2}(C_{22}-C_{23})$$

$$K_{23}=\frac{1}{2}(C_{22}+C_{23})$$

$$E_{22}=E_{33}=\frac{4G_{23}K_{23}}{K_{23}+\psi G_{23}}$$

$$\nu_{21}=\nu_{31}=\nu_1=\frac{1}{2}\left(\frac{C_{11}-E_{11}}{K_{23}}\right)^{1/2}$$

$$\nu_{23}=\frac{K_{23}-\psi G_{23}}{K_{23}+\psi G_{23}}$$

$$\psi=1+\frac{4K_{23}\nu_{12}^2}{E_{11}}$$

Where E_{11} and E_{22} are the equivalent elastic moduli in the x_1 and x_2 directions respectively; G_{12} and ν_{12} are the equivalent shear modulus and equivalent Poisson's ratio in the x_1x_2 plane. G_{23}, K_{23}, and ν_{23} are the equivalent shear modulus, the equivalent volume modulus, and the equivalent Poisson's ratio in the x_2x_3 plane. The coordinate system with axes of x_1, x_2, and x_3 is shown in Fig. 1(a).

Since the representative volume element is regarded as a point with a microstructural homogenized constitutive law, the macro-stress R and the macro-strain Γ are usually defined as the volume average stress in the representative volume element:

$$R=<\sigma>_\Omega=\frac{1}{V_\Omega}\int_\Omega\sigma\mathrm{d}V \text{ and } \Gamma=<\varepsilon>_\Omega=\frac{1}{V_\Omega}\int_\Omega\varepsilon\mathrm{d}V \quad (2)$$

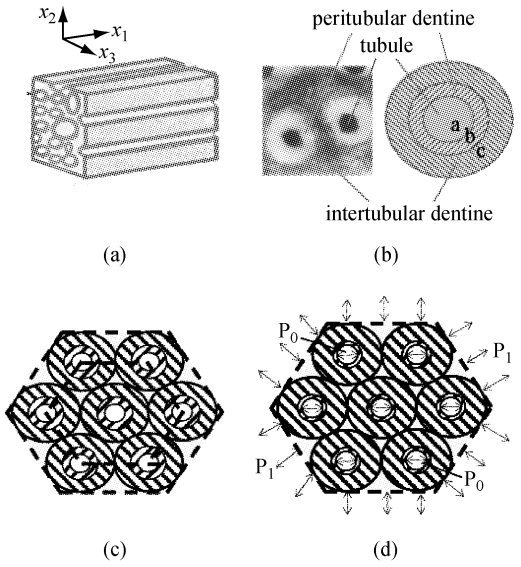

Fig.1 The mechanics model of dentinal microstructures (a) The porous protein-mineral model[6,18], (b) One unit cell of the transverse section of a porous protein-mineral mechanics model, which the left scanned picture was cited from the reference[1-2], (c) A transverse section of a hexagonal representative volume element, (d) A hexagonal model under P_0 and P_1 pressures

图1 牙本质微结构力学模型 (a)蛋白质-矿物质多孔力学模型，(b)蛋白质-矿物质多孔力学模型的1个单元横截面图，左侧扫描图像摘自文献[1-2]，(c)六边形代表体积单元的横截面图，(d)六边形代表体积单元内外压示意图

Where Ω is the domain of the representative volume element and V_Ω represents its volume.

It should be noted that the porous dimension and distribution in dentinal microstructures are sometimes different at different positions or at different ages, and in these cases the computing approaches should be adopted for analysis of the microstructural or macrostructural properties[21].

2 Analyses and Results

2.1 Dependence of micromechanical properties on the tubular direction

Kinney *et al.* have shown the dependence of mechanical properties on the direction of tubules and proposed several laws of angular deviation of tubule based on the experiment[2-3]. Many investigators consider that the tubules rather than the mineralized collagen fibrils are the potential source of elastic anisotropy[22-24]. Micro-hardness, fracture toughness, and cracks of human dentine have been found to be dependent on microstructural orientation of the

teeth[7,25]. Particularly, several micromechanics approaches have been used to discuss the influence of the tubule direction on dentine properties[2,6-8,16-17].

Using the porous protein-mineral micromechanics model, analytic solution of the mechanical properties of microstructural dentine with the tubular direction θ varying from 0° to 90° can be obtained. The constitutive model of the representative volume element expressed by equation (1) can be simplified as following:

$$\begin{Bmatrix}\sigma^1\\ \sigma^2\end{Bmatrix}=\begin{bmatrix}\boldsymbol{C}_1 & 0\\ 0 & \boldsymbol{C}_2\end{bmatrix}\begin{Bmatrix}\varepsilon^1\\ \varepsilon^2\end{Bmatrix} \tag{3}$$

Where $\{\sigma^1\}=\{\sigma_{11}\ \ \sigma_{22}\ \ \sigma_{33}\}^{\mathrm{T}}$, $\{\varepsilon^1\}=\{\varepsilon_{11}\ \ \varepsilon_{22}\ \ \varepsilon_{33}\}^{\mathrm{T}}$, $\{\sigma^2\}=\{\sigma_{23}\ \ \sigma_{31}\ \ \sigma_{12}\}^{\mathrm{T}}$, $\{\varepsilon^2\}=\{\varepsilon_{23}\ \ \varepsilon_{31}\ \ \varepsilon_{12}\}^{\mathrm{T}}$, $\boldsymbol{C}_1=\begin{bmatrix}C_{11} & C_{12} & C_{12}\\ C_{12} & C_{22} & C_{23}\\ C_{12} & C_{23} & C_{22}\end{bmatrix}$ and $\boldsymbol{C}_2=\begin{bmatrix}G_{23} & 0 & 0\\ 0 & C_{44} & 0\\ 0 & 0 & C_{44}\end{bmatrix}$.

If the x_1x_2 plane of the original coordinate system (shown in Fig. 1(a)) is rotated from 0° to θ, and the axis of x_3 is invariant; then in the rotated new coordinate system, the constitutive equation of the representative volume element of dentine microstructure can be expressed as

$$\begin{bmatrix}\sigma^{1\prime}\\ \sigma^{2\prime}\end{bmatrix}=\begin{bmatrix}\boldsymbol{C}_1' & 0\\ 0 & \boldsymbol{C}_2'\end{bmatrix}\begin{bmatrix}\varepsilon^{1\prime}\\ \varepsilon^{2\prime}\end{bmatrix} \tag{4}$$

Where

$$\{\sigma^{1\prime}\}=\{\sigma_{11}'\ \ \sigma_{22}'\ \ \sigma_{33}'\}^{\mathrm{T}}=\boldsymbol{T}\{\sigma^1\}\boldsymbol{T}^{\mathrm{T}}$$

$$\{\varepsilon^{1\prime}\}=\{\varepsilon_{11}'\ \ \varepsilon_{22}'\ \ \varepsilon_{33}'\}^{\mathrm{T}}=\boldsymbol{T}\{\varepsilon^1\}\boldsymbol{T}^{\mathrm{T}}$$

$$\boldsymbol{C}_1'=\boldsymbol{T}\boldsymbol{C}_1\boldsymbol{T}^{\mathrm{T}}$$

$$\boldsymbol{C}_2'=[\boldsymbol{T}][\boldsymbol{C}_2][\boldsymbol{T}]^{\mathrm{T}}$$

$$\boldsymbol{T}=\begin{bmatrix}\cos\theta & -\sin\theta & 0\\ \sin\theta & \cos\theta & 0\\ 0 & 0 & 1\end{bmatrix},\quad \boldsymbol{C}_1'=\begin{bmatrix}C_{11}' & C_{12}' & C_{12}'\\ C_{12}' & C_{22}' & C_{23}'\\ C_{12}' & C_{23}' & C_{22}'\end{bmatrix}$$

$$[C_2']=\begin{bmatrix}G_{23}' & 0 & 0\\ 0 & C_{44}' & 0\\ 0 & 0 & C_{44}'\end{bmatrix}$$

Although it actually has the same format as Eq. (3), equation (4) is only for the situation when θ is varied from 0° to 90°. Thus, the equivalent mechanical properties of dentine microstructure change when the tubular direction θ varies from 0° to 90°.

The variations of equivalent elastic moduli E_{11} and E_{22} with θ under wet and dry situations are presented in Fig. 2 (a) and 2(b) compared with the data obtained from previous experiments[3-4]. The elastic moduli (E_p and E_i) and Poisson's ratio of peritubular dentine and intertubular dentine (ν_p and ν_i) are taken from previous studies[3-4], where $E_p=E_i=24.4$ GPa, $\nu_p=\nu_i=0.29$ for wet situation and $E_p=E_i=28.3$ GPa, $\nu_p=\nu_i=0.28$ for dry situation, and the subscript 'p' and 'i' denote peritubular dentine and intertubular dentine, respectively. It can be seen that the result from theoretical analysis using the porous protein-mineral model is close to those results from experimental studies, though discrepancy does exist.

The equivalent shear moduli G_{12} and G_{23} varying with tubular direction θ under wet and dry conditions are shown in Fig. 2(c); G_{23} gradually increases when θ changes from 0° to 90°, whereas G_{12} reduces a little. The equivalent Poisson's ratio ν_{12} and ν_{23} varying with θ are presented in Fig. 2(d), and ν_{12} gradually increases from 0° to 90°, whereas ν_{23} reduces. Therefore, it can be concluded that the micromechanical properties are dependent on the tubular direction.

2.2 Effect of wet and dry conditions on micromechanics modulus of dentine

It has been reported that the wet and dry conditions cause variations in coefficients of the material properties of dentine specimens[1,3]. The elastic constants for the hexagonal microstructure under wet and dry conditions obtained from the porous protein-mineral model have been compared with those from previous models (Fig. 3)[4-5]. The elastic modulus and Poisson's ratio are taken from previous studies[4-5], where $E_p=28.6$ GPa, $E_i=15.0$ GPa, and $\nu_p=\nu_i=0.25$ are for wet situation, and $E_p=28.6$ GPa, $E_i=20.2$ GPa, and $\nu_p=\nu_i=0.25$ are for dry situation.

The variation of equivalent elastic modulus E_{11} with β and ν_i (Poisson's ratio) for wet and dry situations is shown in Fig. 3(a) and 3(b), respectively, which was cited from the reference[18]. The straight lines in the two figures represent the results obtained from previous model[5], while the parabolic curves represent the results obtained from the current porous protein-mineral model. While the results obtained from previous model show the average value; present model provides a more reasonable solution[5,18].

2.3 Influences of the aging of dentine and the distributions of mineral and collagen on micromechanical properties

With aging, the dentine becomes transparent. Unlike the normal dentine, the transparent dentine exhibits almost no yielding before failure[9], and the flexural strength and

strain of dentine decrease significantly with aging[7,10]. Some studies have revealed that the intertubular mineral crystallites are smaller in transparent dentine[11]. The prediction of the failure behavior of the mineralized tissue is de-

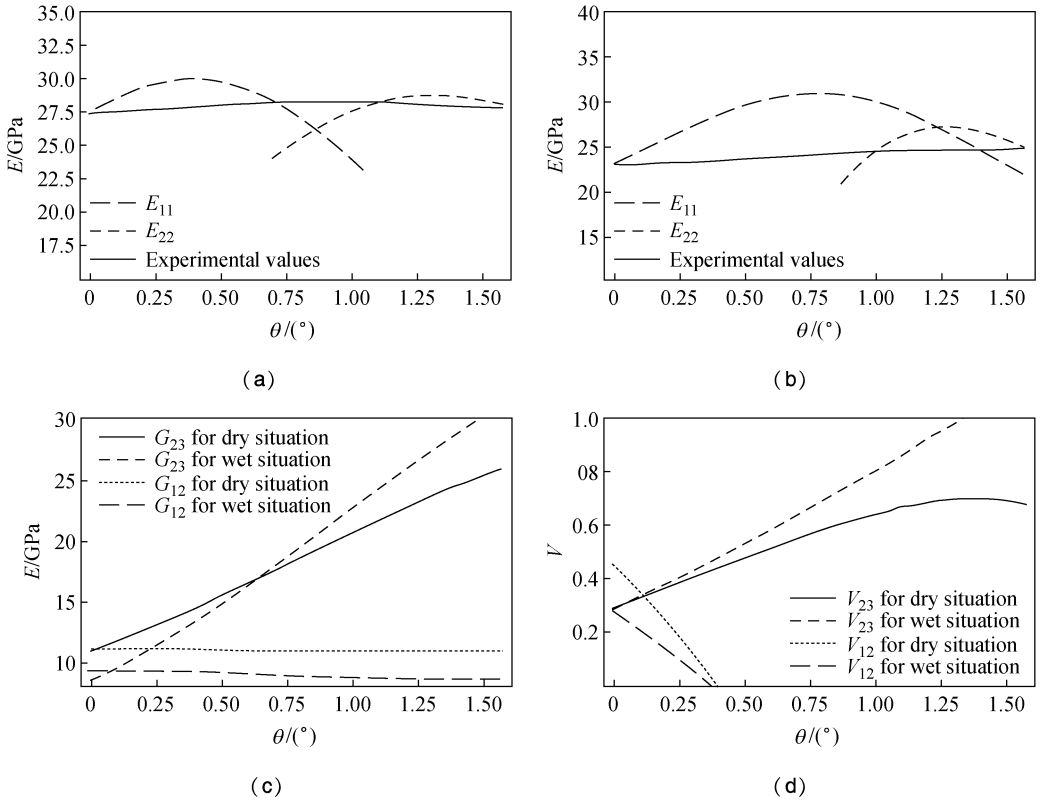

Fig. 2 The relationship between equivalent modulus and tubular direction θ (a) The relationship between the equivalent elastic modulus E and θ for dry situation, (b) The relationship between the equivalent elastic modulus *E* and θ for wet situation, (c) The relationship between the equivalent shear modulus *G* and θ, (d) The relationship between the equivalent Poisson's ratio *ν* and θ

图 2 牙本质微结构等效性质与牙小管方向 θ 的关系图 (a)干燥牙本质的等效弹性模量 E 与牙小管方向 θ 的关系图，(b)湿润牙本质的等效弹性模量 E 与牙小管方向 θ 的关系图，(c)等效剪切模量 G 与牙小管方向 θ 的关系图，(d)等效泊松比 ν 与牙小管方向 θ 的关系图

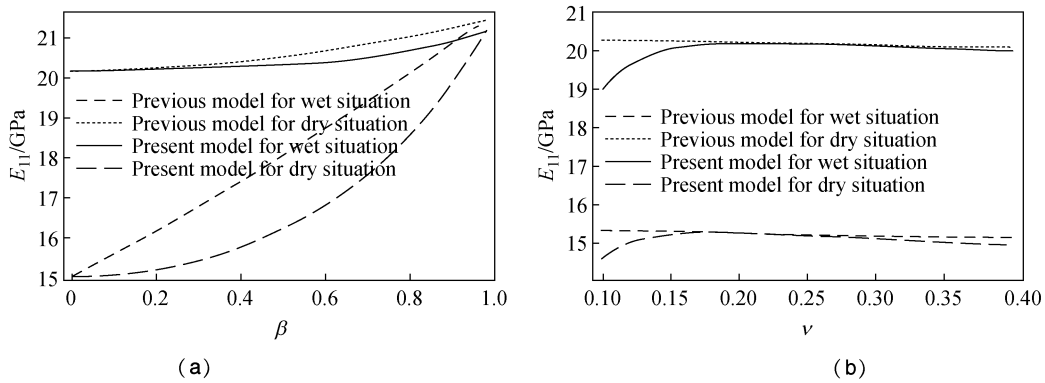

Fig. 3 The relationship between the equivalent modulus and the original parameters under wet and dry conditions (a) The relationship between equivalent elastic modulus E_{11} and β, (b) The relationship between equivalent elastic modulus E_{11} and ν_i (E_p = 28.6 GPa, E_i = 20.2 GPa, and $\nu_p = \nu_i = 0.25$ for dry situation; E_p = 28.6 GPa, E_i = 15.0 GPa, and $\nu_p = \nu_i = 0.25$ for wet situation; $\alpha = 0.5$, $\beta = 0.2$)

图 3 牙本质微结构等效模量与牙本质微结构尺寸性质的关系图 (a)等效弹性模量 E_{11} 与非牙小管所占面积比 β 的关系图，(b)等效弹性模量 E_{11} 与非牙小管泊松比 ν_i 的关系图

veloped from a micromechanics experiment[12]. Based on those experiments[7,9-10], the influences of the aging of dentine and the distributions of mineral and collagen on micromechanical properties model have been discussed using porous protein-mineral herein.

Fig. 4(a) presents the relationship between the equivalent elastic modulus E_{11} and α and β for normal and transparent dentine. The elastic moduli are taken from previous studies[9-10], where $E_{11}=16.7$ GPa and $E_{22}=15.1$ GPa are for a young dentine of a 17-year-old female patient, and $E_{11}=16.9$ GPa and $E_{22}=12.1$ GPa are for an old dentine of a 77-year-old female patient. It can be seen that E_{11} decreases gradually when α and β increase from 0 to 1.0, and E_{11} of the young dentine is always greater than that of the older one. It needs to be noted that E_{11} is almost invariant for the transparent dentine when α changes. The relationship between the equivalent moduli E_{11}, E_i, and E_p for normal and transparent dentine is shown in Fig. 4(b), and it can be seen that E_{11} increases with the increasing of E_i and varies a little with the increasing of E_p.

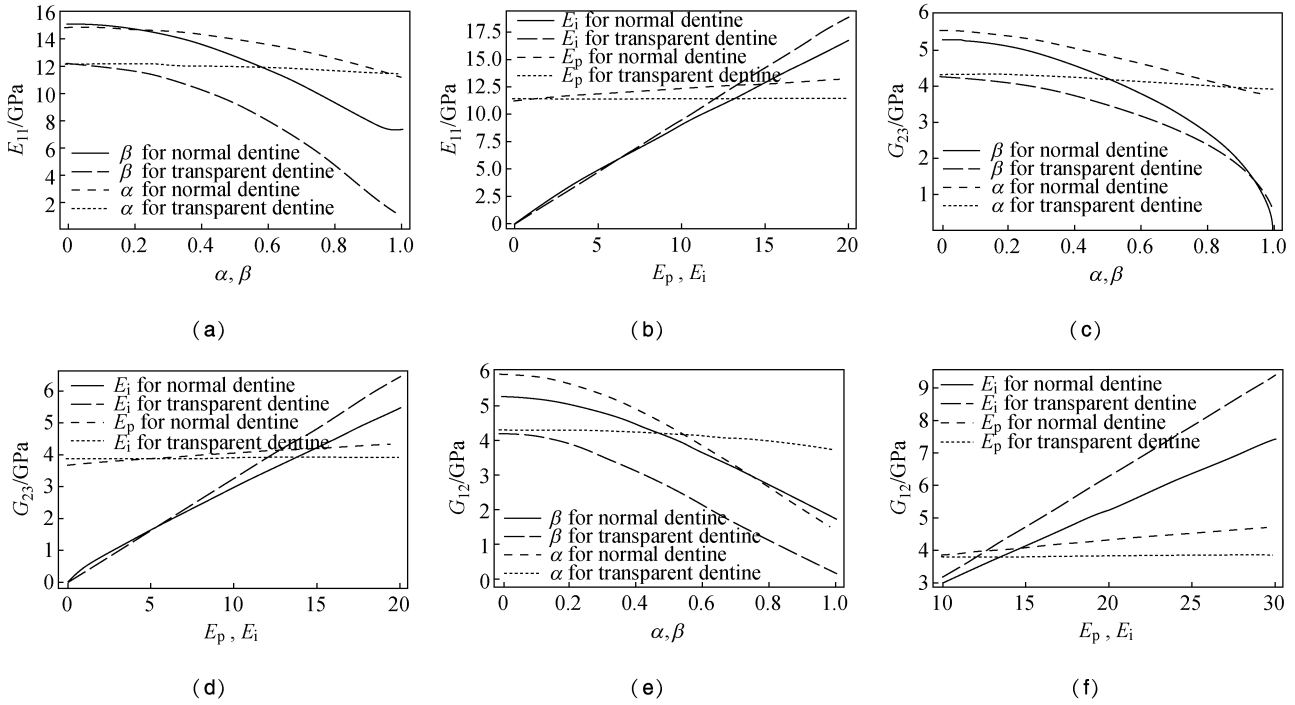

Fig. 4 The relationship between the equivalent modulus and the original parameters for normal and transparent dentine (a) The relationship between the equivalent elastic modulus E_{11} and α and β, (b) The relationship between the equivalent elastic modulus E_{11} and E_p and E_i, (c) The relationship between the equivalent shear modulus G_{23} and α and β, (d) The relationship between the equivalent shear modulus G_{23} and E_p and E_i, (e) The relationship between the equivalent shear modulus G_{12} and α and β, (f) The relationship between the equivalent shear modulus G_{12} and E_p, and E_i.

图4 年青和年老牙本质微结构等效模量与微结构尺寸性质的关系图 (a)等效弹性模量E_{11}与牙小管所占面积比α和非牙小管所占面积比β的关系图,(b)等效弹性模量E_{11}与管周基质模量E_p和管间基质模量E_i的的关系图,(c)等效剪切模量G_{23}与牙小管所占面积比α和非牙小管所占面积比β的关系图,(d)等效剪切模量G_{23}与管周基质模量E_p和管间基质模量E_i的的关系图,(e)等效剪切模量G_{12}与牙小管所占面积比α和非牙小管所占面积比β的关系图,(f)等效剪切模量G_{12}与管周基质模量E_p和管间基质模量E_i的的关系图

The variation of the equivalent shear moduli G_{23} and G_{12} with α and β for normal and transparent dentine are presented in Fig. 4(c) and E, respectively. The global tendency of the results is that G_{23} and G_{12} for transparent dentine are mostly smaller than those for normal dentine, and the values for young dentine are higher than those for the old dentine.

The variation of the equivalent shear moduli G_{23} and G_{12} with E_i and E_p for normal and transparent dentine are plotted in Fig. 4(d) and F. With the increase of E_i, G_{23} is less than G_{12} for both types of dentine, whereas there is no significant difference between G_{23} and G_{12} for both types of

dentine when E_p increases.

2.4 Influence of hydraulic and gas pressure on dentine microstructure

Although some investigations have evaluated the effect of hydraulic pressure on bond strength of dentine composite[26], there are few studies on quantified analysis of this effect. Hence, the influence of hydraulic and gas pressure on dentine microstructure is discussed herein using porous protein-mineral model.

It is well known that the measurement of gas or liquid pressure in dentine microstructure or bone is not an easy task, but it can be hypothesized that a certain gas pressure is equal to 1.0 standard atmospheric pressure (101.3 kPa), and that a certain liquid pressure is equal to a normal blood pressure (for adults, it is 160 mmHg = 210 kPa). Therefore, hydraulic and gas pressure may represent a certain situation for human dentine.

Because the longitudinal size of a cell unit of dentine is always much greater than the size of its transverse part, it can be assumed that the longitudinal displacement w is zero for the representative volume element. Considering the symmetric condition, displacements u_i and stress solution σ_{ij} of the model in column coordinate system can be simplified as following:

$$\left.\begin{aligned} u_r &= \frac{A}{r} + \frac{Br}{C_{22} + C_{23}} \\ u_\theta &= 0 \\ w &= 0 \\ \sigma_z &= C_{11}\varepsilon_z + C_{12}\varepsilon_r + C_{12}\varepsilon_\theta \\ \sigma_r &= C_{12}\varepsilon_z + C_{22}\varepsilon_r + C_{23}\varepsilon_\theta \\ \sigma_\theta &= C_{12}\varepsilon_z + C_{23}\varepsilon_r + C_{22}\varepsilon_\theta \\ \tau_{rz} &= 0 \end{aligned}\right\} \tag{5}$$

where A and B are undetermined constants[18].

Meanwhile, P_0 and P_1 are supposed to be the inside stress of gas and liquid pressures and outside stress caused by the mutual actions among the representative volume elements (as shown in Fig. 1(d)). When the following conditions are satisfied,

$$\left.\begin{aligned} \sigma_r &= -P_0 \text{ at } r = a \\ \sigma_r &= -P_1 \text{ at } r = c \\ u_r &= 0 \text{ at } r = c \end{aligned}\right\} \tag{6}$$

in which a is the radius of the tubules, and c is the radius of the intertubule dentine, we have

$$\left.\begin{aligned} P_1 &= \frac{2a^2C_{22}P_0}{a^2C_{22} + a^2C_{23} + c^2C_{22} - c^2C_{23}} \\ A &= \frac{a^2c^2P_0}{a^2C_{22} + a^2C_{23} + c^2C_{22} - c^2C_{23}} \\ B &= \frac{a^2P_0(C_{22} + C_{23})}{a^2C_{22} + a^2C_{23} + c^2C_{22} - c^2C_{23}} \\ \sigma_r &= \frac{-\alpha^2P_0(C_{22} - C_{23} + \beta^2C_{22} + \beta^2C_{23})}{C_{22} - C_{23} + \alpha^2\beta^2C_{22} + \alpha^2\beta^2C_{23}} \\ \sigma_\theta &= \frac{-\alpha^2P_0(-C_{22} + C_{23} + \beta^2C_{22} + \beta^2C_{23})}{C_{22} - C_{23} + \alpha^2\beta^2C_{22} + \alpha^2\beta^2C_{23}} \\ \sigma_z &= \frac{-\alpha^2\beta^2C_{12}P_0}{C_{22} - C_{23} + \alpha^2\beta^2C_{22} + \alpha^2\beta^2C_{23}} \end{aligned}\right\} \tag{7}$$

where $\alpha = a/r$ and $\beta = r/c$ are the same as the variables mentioned before.

Equation (7) shows the variation of the stresses of the representative volume element of dentine microstructure with α and β respectively. The absolute values of all three stresses increase when β goes up, and significant change of stress value of σ_θ and σ_r exists; however, little change is observed in the value of σ_z. For example, the largest pressure value, which can be caused by normal blood pressure and standard atmospheric pressure is about 0.05 MPa when $\alpha = 0.4$; while the smallest value is close to 0 MPa. The maximal values are reduced when α decreases.

3 Conclusions

A porous protein-mineral mechanics model has been used to evaluate the mechanical properties and interacting mechanism for the dentine microstructure in this study. The dentine microstructure is assumed to be in hexagonal shape, and the interactions among the tubules, the peritubular and intertubular dentinal matrix, have been taken into account in the present model. The constitutive relationship of representative volume element is assumed based on a transversely isotropic model in light of experimental investigations.

The following conclusions are drawn from this study:

(1) The consistency between result from theoretical analysis using porous protein-mineral model and result from the experimental studies demonstrates the accuracy and efficiency of the porous protein-mineral model.

(2) The variation of the effective elastic constants of micromechanics model with the tubular direction varying from 0° to 90° demonstrates the significant influence of tubular direction on the dentinal micromechanical properties.

(3) The porous protein-mineral model can describe the properties of micromechanics of dentine more effectively than previous model that provides only an average value.

(4) The effective elastic constants of the dentine microstructure vary with the aging and the distributions of mineral and collagen.

(5) The influence of hydraulic and gas pressure on dentine microstructure can be evaluated using porous protein-mineral model, and the absolute values of the stresses of hydraulic and gas tubular pressure σ_r and σ_θ increase in association with the increase of α. The largest pressure value, which is caused by normal blood pressure and standard atmospheric pressure, is about 0.05 MPa when $\alpha = 0.4$, and the maximal values are reduced when α decreases.

References:

[1] Kinney JH, Marshal SJ, Marshall GW. The mechanical properties of human dentin: A critical review and re-evaluation of the dental literature[J]. Crit Rev Oral Bio Med, 2003, 14(1): 13-29.

[2] Marshall GW Jr, Marshall SJ, Kinney JH, *et al.* The dentin substrate: Structure and properties related to bonding[J]. J Dent, 1997, 25(6): 441-458.

[3] Kinney JH, Gladden JR, Marshall GW, *et al.* Resonant ultrasound spectroscopy measurements of the elastic constants of human dentin[J]. J Biomech, 2004, 37(4): 437-441.

[4] Pashley DA. Dentin: A dynamic substrate-a review[J]. Scan Micros, 1989, 3(1): 161-176.

[5] Kinney JH, Balooch M, Marshall GW, *et al.* A micromechanics model of the elastic properties of human dentin[J]. Arch Oral Biol, 1999, 44(10): 813-822.

[6] Huo B, Zheng QS. Effect of dentin tubules on the mechanical properties of dentin, Part I: Stress-strain relations and strength criterion[J]. Acta Mechanica Sinica, 1999, 15(4): 355-365.

[7] Arola DD, Reprogel RK. Tubule orientation and the fatigue strength of human dentin[J]. Biomaterials, 2006, 27(9): 2131-2140.

[8] Qin QH, Swain MV. A micro-mechanics model of dentin mechanical properties[J]. Biomaterials, 2004, 25(20): 5081-5090.

[9] Kinney JH, Nalla RK, Pople JA, *et al.* Age-related transparent root dentin: mineral concentration, crystallite size, and mechanical properties[J]. Biomaterials, 2005, 26(16): 3363-3376.

[10] Arola DD, Reprogel RK. Effects of aging on the mechanical behavior of human dentin[J]. Biomaterials, 2005, 26(18): 4051-4061.

[11] Porter AE, Nalla RK, Minor A, *et al.* A transmission electron microscopy study of mineralization in age-induced transparent dentin[J]. Biomaterials, 2005, 26(36): 7650-7660.

[12] Nalla RK, Porter AE, Daraio C, *et al.* Ultrastructural examination of dentin using focused ion-beam cross-sectioning and transmission electron microscopy[J]. Micron, 2005, 36(7-8): 672-680.

[13] Christensen RM, Lo KH. Solution for effective shear properties in three phase sphere and cylinder models[J]. J Mech Phys Solids, 1979, 27(4): 315-330.

[14] Christensen RM. A critical evaluation for a class of micromechanics models[J]. J Mech Phys Solids, 1990, 38(3): 379-404.

[15] Katz JL. Hard tissue as a composite material—I bounds on the elastic behaviour[J]. J Biomech, 1971, 4(5): 455-73.

[16] Huo B, Zheng QS, Zhang Q, *et al.* Effect of dentintubules to the mechanical properties of dentin: Part II experimental study[J]. Acta Mechanica Sinica, 2000, 16(1): 75-82.

[17] Hashin Z, Rosen BW. The elastic moduli of fiber-reinforced materials[J]. J Applied Mech, 1964, 31: 223-232.

[18] Cui YH, Wang X, Zhang YX, *et al.* Poroelastic properties of anisotropic cylinder composite materials[J]. Philosophical Magazine Letters, 2008, 88: 767-783.

[19] Cui YH, Wang X, Zhang YX, *et al.* Poro-viscoelastic properties of anisotropic cylindrical composite materials[J]. Philos Mag, 2010, 90(9): 1197-1212.

[20] Jones B, Boyde A. Ultrastructure of dentin and dentinogenesis. In: Dentin and Dentinogenesis[M]. Boca Raton: CRC Press, 1984: 81-134.

[21] Wang JG, Leungb CF, Ichikawac Y. A simplified homogenisation method for composite soils[J]. Comput Geotech, 2002, 29(6): 477-500.

[22] Currey JD. The design of mineralized hard tissues for their mechanical functions[J]. J Exp Biol, 1999, 202(23): 3285-3294.

[23] Mann S, Weiner SB. Biomineralization: Structural questions at all length scales[J]. J Struct Biol, 1999, 126(3): 179-181.

[24] Weiner S, Traub W, Wagner HD. Lamellar bone: Structure function relations[J]. J Struct Biol, 1999, 126(3): 241-255.

[25] Saker-Deliormanli A, Giiden M. Microhardness and fracture toughness of dental materials by indentation method[J]. J Biomed Mater Res B Appl Biomater, 2006, 76(2): 257-264.

[26] Zheng L, Pereira PN, Somphone P, *et al.* Effect of hydrostatic pressure on regional bond strengths of compomers to dentinev[J]. J Dent, 2000, 28(7): 501-508.